

Structure and Activity Peculiarities of Ruthenium Quinoline and Quinoxaline Complexes: Novel Metathesis Catalysts

Michał Barbasiewicz,* Anna Szadkowska, Robert Bujok, and Karol Grela*

Institute of Organic Chemistry, Polish Academy of Sciences, Kasprzaka 44/52, 01-224 Warsaw, Poland

Received January 29, 2006

Novel metathesis catalysts that are derivatives of 8-vinylquinoline, $(\text{H}_2\text{IMes})(\text{Cl})_2\text{Ru}(\text{CH}-\kappa^2(\text{C},\text{N})\text{-}8\text{-C}_9\text{H}_6\text{N})$ (**1a**; $\text{H}_2\text{IMes} = 1,3\text{-dimesityl-}4,5\text{-dihydroimidzol-}2\text{-ylidene}$), and 5-vinylquinoxaline, $(\text{H}_2\text{IMes})(\text{Cl})_2\text{Ru}(\text{CH}-\kappa^2(\text{C},\text{N})\text{-}5\text{-C}_8\text{H}_5\text{N}_2)$ (**2a**), which possess five-membered chelate rings, were synthesized in ligand exchange reactions with $(\text{H}_2\text{IMes})(\text{PCy}_3)(\text{Cl})_2\text{Ru}=\text{CHPh}$. Both **1a** and **2a** are formed as complexes with the *trans*-dichloro geometry common for Grubbs-type complexes, while on prolonged storage in dichloromethane they isomerize to the thermodynamically favored *cis*-dichloro isomers (**1b** and **2b**, respectively). The structures of compounds **1a,b** were confirmed by X-ray analysis. The kinetics of *trans* to *cis* isomerization were measured by ^1H NMR to give the rate constants $k_{1\text{a}\rightarrow 1\text{b}} = 3.2 \times 10^{-2} \text{ h}^{-1}$ and $k_{2\text{a}\rightarrow 2\text{b}} = 5.5 \times 10^{-3} \text{ h}^{-1}$ in dichloromethane- d_2 at 23 °C. Investigations of the relative activities of these catalysts in model RCM and enyne reactions showed that catalyst **1a** was faster than **1b** (and **2a** faster than **2b**) but that **2a** was faster than **1a**.

Introduction

Over the past decade olefin metathesis has experienced dramatic development as a useful tool for the formation of C=C bonds in organic synthesis and polymer science.¹ A continuous survey across the structures has led to the development of highly active catalysts for sophisticated synthetic tasks and more stable ones for polymer technology (so-called “latent” catalysts).² The latter often exhibit decreased initiation rates in ring-opening olefin metathesis polymerization, which can allow for longer handling of a monomer–catalyst mixture before the polymerization starts.^{2,3}

In both groups of Ru complexes a wise choice of chelating ligands plays a predominant role, while their activity can later be fine-tuned by the introduction of substituents and relevant changes in the geometry of the complexes. These compounds can be generally classified according to the type of donor atom forming a chelate with a Ru alkylidene (carbene) fragment. Oxygen ether derivatives (e.g. **I**; Figure 1), pioneered by Hoveyda,⁴ exhibit high activity and possess excellent functional group tolerance. The Ru–O chelate can easily dissociate and release active 14-electron ruthenium complexes, the intrinsic catalytic intermediates.⁴ Catalyst **I** was later successfully fine-tuned in order to increase its activity and applicability by the introduction of electron-withdrawing groups to diminish the donor properties of the oxygen atom.^{5,6} Otherwise, oxygen carbonyl donors, e.g. 2-vinylbenzoic acid derivatives (**II**; L = PCy_3 , 1,3-dimesitylimidazol-2-ylidene), are less reactive in the

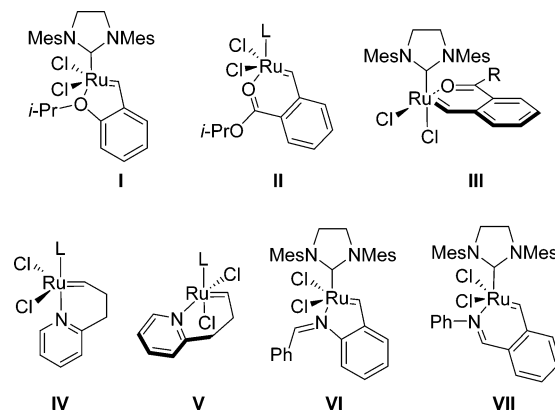


Figure 1. Representative *O*- and *N*-ruthenium chelates exhibiting activity in olefin metathesis (Mes = 2,4,6-trimethylphenyl, Cy = cyclohexyl).

RCM of substituted dienes.⁷ All these compounds have in common a square-pyramidal *trans*-dichloro geometry (*SPY*-5-31), where the carbon atom of the NHC ligand, chloride ions, and the oxygen atom of the chelate lie in one plane and the alkylidene substituent occupies the perpendicular position. An interesting variation from this structure, which exhibited a *cis*-dichloro orientation (*SPY*-5-34), was observed initially for η^3 -vinylcarbene complexes by Grubbs.⁸ Slugovc⁹ described similar Hoveyda-type *cis*-dichloro complexes (**III**) with a chelating

* To whom correspondence should be addressed. E-mail: barabasz@icho.edu.pl (M.B.); grela@icho.edu.pl (K.G.).

(1) *Handbook of Metathesis*; Grubbs, R. H., Ed.; Wiley-VCH: Weinheim, Germany, 2003; Vols. 1–3.

(2) Ung, T.; Hejl, A.; Grubbs, R. H.; Schrod, Y. *Organometallics* **2004**, *23*, 5399.

(3) Slugovc, C.; Burtscher, D.; Stelzer, F.; Mereiter, K. *Organometallics* **2005**, *24*, 2255.

(4) (a) Harrity, J. P. A.; La, D. S.; Cefalo, D. R.; Visser, M. S.; Hoveyda, A. H. *J. Am. Chem. Soc.* **1998**, *120*, 2343. (b) Kingsbury, J. S.; Harrity, J. P. A.; Bonitatebus, P. J., Jr.; Hoveyda, A. H. *J. Am. Chem. Soc.* **1999**, *121*, 791. (c) Garber, S. B.; Kingsbury, J. S.; Gray, B. L.; Hoveyda, A. H. *J. Am. Chem. Soc.* **2000**, *122*, 8168.

(5) (a) Grela, K.; Harutyunyan, S.; Michrowska, A. *Angew. Chem.* **2002**, *114*, 4210; *Angew. Chem., Int. Ed.* **2002**, *41*, 4038. (b) Harutyunyan, S.; Michrowska, A.; Grela, K. A Highly Active Ruthenium (Pre)catalyst for Metathesis Reactions. In *Catalysts for Fine Chemical Synthesis*; Roberts, S. M., Whittall, J., Mather, P., McCormack, P., Eds.; Wiley: New York, 2004; Vol. 3 (Metal Catalysed Carbon–Carbon Bond-Forming Reactions), Chapter 9.1, pp 169–173. (c) Gułajski, L.; Michrowska, A.; Bujok, R.; Grela, K. *J. Mol. Catal. A: Chem.*, in press.

(6) Michrowska, A.; Bujok, R.; Harutyunyan, S.; Sashuk, V.; Dolgonos, G.; Grela, K. *J. Am. Chem. Soc.* **2004**, *126*, 9318.

(7) Fürstner, A.; Thiel, O. R.; Lehmann, C. W. *Organometallics* **2002**, *21*, 331.

(8) For some earlier examples of *cis*-dichloride complexes, see: Trnka, T. M.; Day, M. W.; Grubbs, R. H. *Organometallics* **2001**, *20*, 3845 and references therein.

carbonyl group, which catalyzed the ROMP polymerization of functionalized norbornenes.¹⁰

To the second group of complexes belong chelates formed via nitrogen donor atoms.¹¹ Phosphine-based derivatives of 2-(3-butenyl)pyridine, introduced by van der Schaaf¹² (**IV**; L = P(*i*-Pr)₃) were tested in ROMP, where desired gel times and initiation temperatures were tuned by changing the substitution pattern of the pyridine ring. Later, Schrodi² demonstrated an analogous NHC derivative, which exhibited the aforementioned isomerism. The *trans*-dichloro complex **IV** (L = H₂IMes), initially formed by a ligand exchange procedure from (H₂IMes)(py)₂(Cl)₂Ru=CHPh, slowly converted into the *cis* isomer **V** (L = H₂IMes), while on prolonged heating in a solution a ~3:7 equilibrium between these complexes was established. Recently, Slugovc³ also explored five- and six-membered imine chelates (**VI**, **VII**) and studied the influence of the chelating carbene ring size on the ROM polymerization activity of these catalysts.¹³

New Quinoline and Quinoxaline Complexes: Synthesis, Isomerization, and X-ray Structures

Our present work has been aimed at preparing a novel group of quinoline and quinoxaline-derived ruthenium complexes, bearing a saturated NHC ligand. Unlike the recent approach of Slugovc,³ we decided to apply in our studies quinoline and quinoxaline structural motifs to form more rigid analogues of the rather flexible five-membered imine chelate **VII**.¹⁴

Complexes **1a** and **2a** were conveniently obtained from the Grubbs second-generation catalyst (H₂IMes)(PCy₃)(Cl)₂Ru=CHPh and vinyl-substituted quinoline and quinoxaline via a ligand exchange procedure. 8-Vinylquinoline can be obtained from 8-hydroxyquinoline in a two-step synthesis consisting of formation of a triflate ester¹⁵ and the subsequent Stille reaction with tributylvinylstannane in a procedure analogous to that described in the literature.¹⁶ Similarly, 5-vinylquinoxaline was synthesized from quinoxaline via bromination¹⁷ and a Stille reaction (Figure 2).¹⁸

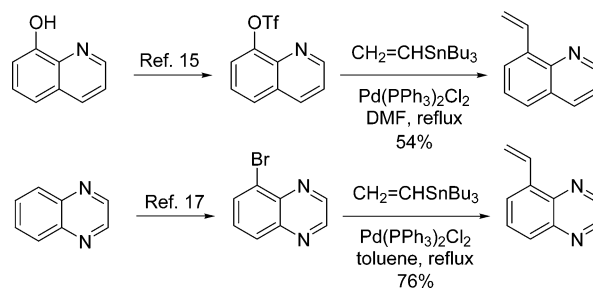


Figure 2. Synthesis of 8-vinylquinoline and 5-vinylquinoxaline.

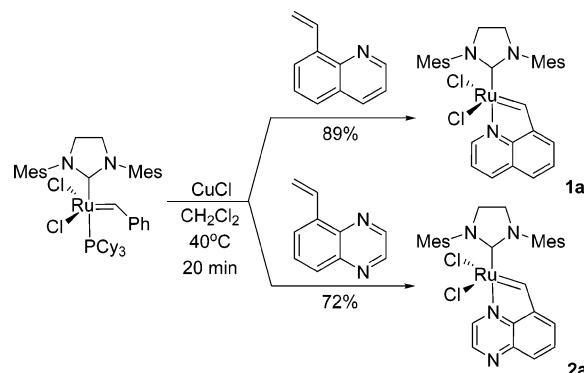


Figure 3. Formation of complexes **1a** and **2a** via a ligand exchange procedure.

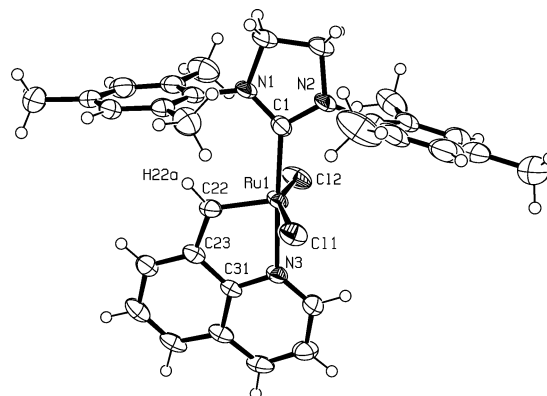


Figure 4. ORTEP²⁰ drawing of **1a** (*trans*-dichloro) (**1a**-C₆H₆; the cocrystallized solvent molecule has been omitted for clarity) represented by thermal ellipsoids drawn at the 50% probability level. Selected bond distances (Å) and angles (deg): Ru(1)–C(1) = 2.063(4), Ru(1)–C(22) = 1.845(4), Ru(1)–N(3) = 2.162(3), Ru(1)–Cl(1) = 2.3519(10), Ru(1)–Cl(2) = 2.3465(10); Cl(1)–Ru(1)–Cl(2) = 155.48(5), C(1)–Ru(1)–N(3) = 176.37(12), C(22)–Ru(1)–N(3) = 80.55(14), C(1)–Ru(1)–Cl(2) = 89.69(11), Cl(1)–Ru(1)–N(3) = 86.70(8).

Ligand exchange proceeded cleanly in the presence of CuCl in dichloromethane at 40 °C within 20 min to give complexes **1a** and **2a** in high yields (Figure 3).

The prepared complexes **1a** and **2a** were perfectly stable and air-tolerant. The ruthenium carbene catalyst **1a** was characterized by NMR and appears to be a complex with *C_s* symmetry (Cl–Ru–Cl *trans*).¹⁹ The carbene proton resonance appeared at 17.06 ppm (in CDCl₃). Crystals suitable for X-ray analysis were obtained from a mixture of benzene and *n*-hexane. The molecular structure of **1a** in the solid state (Figure 4) was in excellent agreement with the *C_s*-symmetric structure deduced from the NMR data.

(19) For a discussion of ¹H NMR spectra of similar isomeric complexes see ref 2.

(9) Slugovc, C.; Perner, B.; Stelzer, F.; Mereiter, K. *Organometallics* **2004**, *23*, 3622.

(10) For similar *trans* to *cis* rearrangements of nonchelating ligands on silica gel, see: Prühs, S.; Lehmann, C. W.; Fürstner, A. *Organometallics* **2004**, *23*, 280.

(11) (a) For complexes bearing chelating pyridinyl–alcoholato ligands, see: Denk, K.; Fridgen, J.; Herrmann, W. A. *Adv. Synth. Catal.* **2002**, *344*, 666. (b) Cationic and neutral ruthenium vinylidene complexes containing tridentate pyridine ligands: Del Rio, R.; Van Koten, G. *Tetrahedron Lett.* **1999**, *40*, 1401. (c) For neutral and cationic Ru tris(pyrazolyl)borate alkylidene and vinylidene complexes, see: Sanford, M. S.; Henling, L. M.; Grubbs, R. H. *Organometallics* **1998**, *17*, 5384. (d) Katayama, H.; Yoshida, T.; Osawa, F. *J. Organomet. Chem.* **1998**, *52*, 203.

(12) van der Schaaf, P. A.; Kolly, R.; Kimer, H.-J.; Rime, F.; Mühlbach, A.; Hafner, A. *J. Organomet. Chem.* **2000**, *606*, 65.

(13) For other Ru complexes, containing Schiff base ligands, see: (a) Chang, S.; Jones, L.-R., II; Wang, C.; Henling, L. M.; Grubbs, R. H. *Organometallics* **1998**, *17*, 3460. (b) De Clercq, B.; Verpoort, F. *Adv. Synth. Catal.* **2002**, *344*, 639. (c) De Clercq, B.; Verpoort, F. *J. Mol. Catal. A: Chem.* **2002**, *180*, 67. (d) Opstal, T.; Verpoort, F. *Angew. Chem., Int. Ed.* **2003**, *42*, 2876. (e) Opstal, T.; Verpoort, F. *Synlett* **2002**, 935. (f) De Clercq, B.; Lefebvre, F.; Verpoort, F. *Appl. Catal. A: Gen.* **2003**, *247*. (g) De Clercq, B.; Lefebvre, F.; Verpoort, F. *New J. Chem.* **2002**, *26*, 1201.

(14) The PhCH=NPh motif within the catalyst structure, described in ref 3, was twisted by about 30° for the five-membered-ring chelate complex.

(15) (a) Stille, J. K.; Echavarran, A. M. *J. Am. Chem. Soc.* **1987**, *109*, 5478. (b) 8-Quinolinyl triflate is commercially available from Aldrich Inc.

(16) The reaction was performed according to the procedure described in: Crisp, G. T.; Papadopoulos, S. *Aust. J. Chem.* **1989**, *42*, 279.

(17) Brown, W. D.; Gouliavaev, A. H. *Synthesis* **2002**, 83.

(18) The reaction was performed according to the procedure described in: van Mullekom, H. A. M.; Vekemans, J. A. J. M.; Meijer, E. W. *Chem. Eur. J.* **1998**, *4*, 1235.

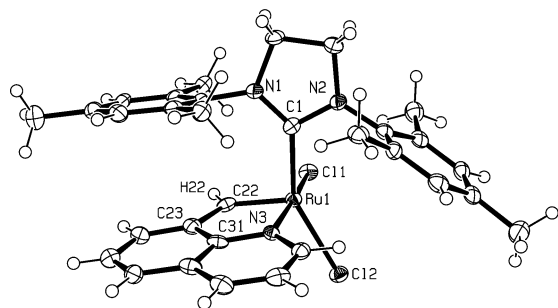


Figure 5. ORTEP²⁰ drawing of **1b** (*cis*-dichloro) represented by thermal ellipsoids drawn at the 50% probability level. Selected bond distances (Å) and angles (deg): Ru(1)–C(1) = 2.008(4), Ru(1)–C(22) = 1.823(4), Ru(1)–N(3) = 2.072(3), Ru(1)–Cl(1) = 2.3812(10), Ru(1)–Cl(2) = 2.3731(10); Cl(1)–Ru(1)–Cl(2) = 89.61(3), C(1)–Ru(1)–N(3) = 96.82(13), C(22)–Ru(1)–N(3) = 81.73(15), C(1)–Ru(1)–Cl(2) = 150.36(11), Cl(1)–Ru(1)–N(3) = 171.52(9).

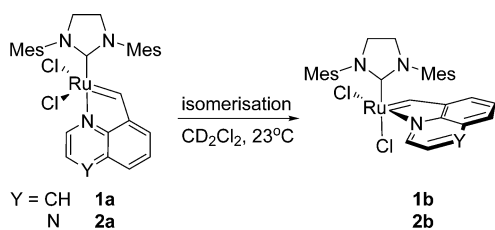


Figure 6. Isomerization process.

Monitoring the reaction of the second-generation Grubbs catalyst with 8-vinylquinoline (Figure 3) by ¹H NMR revealed that the production of **1a** was followed by the slow formation of a different complex (**1b**), exhibiting a carbene proton resonance at 17.45 ppm (in CDCl₃). When a solution of **1a** was left in an NMR tube for 4 days at room temperature, a 22:78 mixture of **1a,b** was obtained. The major isomer was separated by two consecutive crystallizations from ethyl acetate–pentane and dichloromethane–pentane mixtures. According to ¹H NMR the new complex **1b** appeared to be of C₁ symmetry (Cl–Ru–Cl *cis*), which was later confirmed by an X-ray analysis of the solid-state structure (Figure 5).

From the results summarized above, it can be deduced that complexes **1a,b** show structural features similar to those reported for the second-generation pyridine complexes **IV** and **V** bearing a six-membered metallacycle.²

The quinoxaline-based catalyst **2a** was slightly less stable than **1a**, decomposing slowly in CDCl₃ solution, probably due to traces of acid present commonly in this solvent,²¹ but seemed to be very stable in CD₂Cl₂. Its ¹H NMR spectrum indicated a C_s-symmetric complex (Cl–Ru–Cl *trans*) with a carbene proton resonance at 17.10 ppm (in CDCl₃).

Since isomerization processes were precedented,^{2,3} the reasonable stability of these complexes encouraged us to measure the kinetics of their isomerization on the basis of ¹H NMR integration of characteristic benzylidene protons. We chose dichloromethane, assumed to be an excellent solvent for this purpose (Figure 6).²²

(20) We wish to acknowledge for use of a free version of Ortep-3 for Windows program: Farrugia, L. J. *J. Appl. Crystallogr.* **1997**, *30*, 565.

(21) Isomerization of **2a** in CDCl₃ was very slow, and only traces of **2b** were detected in NMR samples on prolonged storage. However, we undoubtedly identified **2b** in a mixture with **2a** in CD₂Cl₂. Ru=CH carbene proton resonances (¹H NMR, CD₂Cl₂): δ 17.13 (**1a**), 17.47 (**1b**), 17.02 (**2a**), 17.29 ppm (**2b**).

(22) Benitez, D.; Goddard, W. A. *J. Am. Chem. Soc.* **2005**, *127*, 12218.

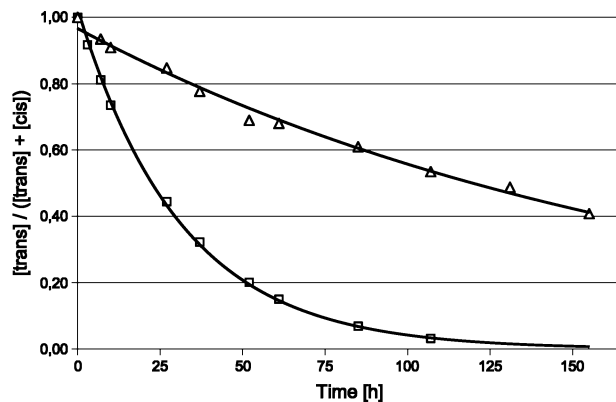


Figure 7. Kinetics of isomerization (according to ¹H NMR) of **1a** to **1b** (□) and of **2a** to **2b** (Δ) in CD₂Cl₂ at 23 °C. Data were fitted with an exponential equation (plot), with correlation coefficients $R^2_{1a-1b} = 0.9994$ and $R^2_{2a-2b} = 0.9927$ and calculated rate constants $k_{1a-1b} = 3.2 \times 10^{-2} \text{ h}^{-1}$ and $k_{2a-2b} = 5.5 \times 10^{-3} \text{ h}^{-1}$.

substrate	product	catalyst	yield (GC)
 4a	 4b	1a	32%
		1b	14%
		2a	38%
		2b	18%
 5a	 5b	1a	41%
		1b	22%
		2a	56%
		2b	29%
 6a	 6b	1a	64%
		1b	51%
		2a	72%

Figure 8. Catalytic activity of **1a,b** and **2a,b** in RCM reactions of model substrates (dichloromethane, room temperature, 24 h; conversions according to GC).

The results of these experiments are presented in Figure 7. While the quinoline complex **1a** isomerized completely (as detected by ¹H NMR) to the *cis* species **1b** within about 6 days at 23 °C,²³ the quinoxaline complex **2a** was significantly less prone to isomerization. However, the experimental data fitted with an exponential equation—common for a first-order isomerization process—showed that the equilibrium of this process also has to be substantially moved to the right. It should be noted that even after prolonged storage of **1a** and **2a** solutions we observed only minute amounts of decomposition products. This corroborates the high stability of these complexes both in the solid form as well as in solution.

Reactivity of New Catalysts

Three model RCM and enyne metathesis reactions were used as a test to compare the activity of catalysts **1a,b** and **2a,b**, as presented in Figures 8 and 9. Typically 5% mol of the catalyst was added to a solution of substrate in CH₂Cl₂ and the reaction was run at room temperature under argon for 24 h. For the RCM of diallyl diethylmalonate (**4a**) samples were taken during the reaction to control the progress in time (Figure 9). Crude reaction mixtures containing an internal standard were analyzed by gas chromatography.

In all model reactions catalyst **1a** was faster than **1b** (and **2a** faster than **2b**), but **2a** was faster than **1a**. The difference in activity between **1a** and **1b** (**2a** and **2b**, respectively) can be

(23) In an independent experiment a pure sample of **1b** dissolved in CD₂Cl₂ gave no detectable Ru=CH NMR signal for **1a** (17.13 ppm), even on prolonged equilibration.

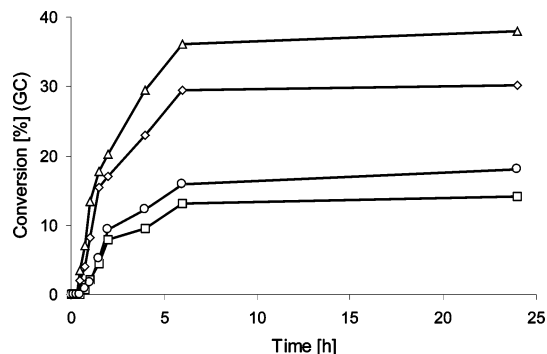


Figure 9. Catalytic activity of **1a** (◇), **1b** (□), **2a** (△), and **2b** (○) in RCM of diallyl diethylmalonate (**4a** → **4b**; dichloromethane, room temperature, 24 h; conversions according to GC).

attributed to the fact that the quinoline ligand in **1a** and **2a** is located trans to the strongly σ -donating NHC ligand and therefore dissociates more quickly to give catalytically active 14-electron species than in the case of **1b** and **2b**.²⁴

Discussion

The presented results show some unexpected features of these compounds. The quinoline derivative **1a** exhibits catalytic activity lower than that of the quinoxaline complex **2a**. At the same time, the rates of their isomerization are reversed—**1a** is completely transformed into **1b** within a few days, while **2a** has a similar half-life. These apparent discrepancies can be rationalized in terms of the influence of electronic effects of a donor atom on the chelate stability, the phenomena previously applied by us for activation of the Hoveyda catalyst **I**.^{5,6} To compare the properties of quinoline and quinoxaline ligands in more detail, we calculated^{25,26} the structures of 8-vinylquinoline and 5-vinylquinoxaline (precursors of the carbene ligands of **1a** and **2a**) and studied their geometries and electron distribution (viewed as EPS charges located at the chelating nitrogen atoms; Figure 10).⁶

This simplified approach showed very similar geometries for these compounds, while important differences in their electronic distribution were found. As the electron density on chelating heteroatoms governs the initiation rate of the complexes,⁶ the more nucleophilic quinoline ligand, which possesses a greater negative charge at nitrogen (−0.410), should exhibit lower activity than quinoxaline (−0.197), as was indeed observed in this case. Strong support for this hypothesis was given by

(24) A similar rationalization was presented in ref 2.

(25) Frisch, M. J.; Trucks, G. W.; Schlegel, H. B.; Scuseria, G. E.; Robb, M. A.; Cheeseman, J. R.; Montgomery, J. A., Jr.; Vreven, T.; Kudin, K. N.; Burant, J. C.; Millam, J. M.; Iyengar, S. S.; Tomasi, J.; Barone, V.; Mennucci, B.; Cossi, M.; Scalmani, G.; Rega, N.; Petersson, G. A.; Nakatsuji, H.; Hada, M.; Ehara, M.; Toyota, K.; Fukuda, R.; Hasegawa, J.; Ishida, M.; Nakajima, T.; Honda, Y.; Kitao, O.; Nakai, H.; Klene, M.; Li, X.; Knox, J. E.; Hratchian, H. P.; Cross, J. B.; Bakken, V.; Adamo, C.; Jaramillo, J.; Gomperts, R.; Stratmann, R. E.; Yazyev, O.; Austin, A. J.; Cammi, R.; Pomelli, C.; Ochterski, J. W.; Ayala, P. Y.; Morokuma, K.; Voth, G. A.; Salvador, P.; Dannenberg, J. J.; Zakrzewski, V. G.; Dapprich, S.; Daniels, A. D.; Strain, M. C.; Farkas, O.; Malick, D. K.; Rabuck, A. D.; Raghavachari, K.; Foresman, J. B.; Ortiz, J. V.; Cui, Q.; Baboul, A. G.; Clifford, S.; Cioslowski, J.; Stefanov, B. B.; Liu, G.; Liashenko, A.; Piskorz, P.; Komaromi, I.; Martin, R. L.; Fox, D. J.; Keith, T.; Al-Laham, M. A.; Peng, C. Y.; Nanayakkara, A.; Challacombe, M.; Gill, P. M. W.; Johnson, B.; Chen, W.; Wong, M. W.; Gonzalez, C.; Pople, J. A. *Gaussian 03*, revision B.05; Gaussian, Inc.: Wallingford, CT, 2004.

(26) All of the calculations were performed using Gaussian 03. The structures of 8-vinylquinoline and 5-vinylquinoxaline were optimized using B3LYP with the 6-31G** basis set in the gas phase. Only real values of the analytical harmonic vibrational frequencies confirmed that the geometries under study correspond to the minimum-energy structures.

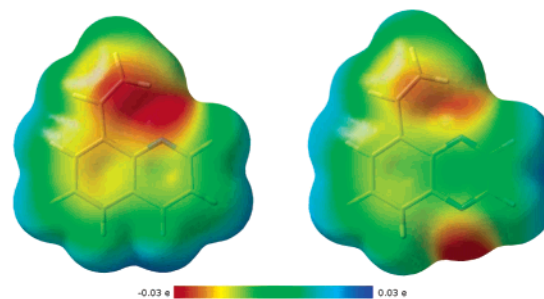


Figure 10. Structures of 8-vinylquinoline (left) and 5-vinylquinoxaline (right) optimized^{25,26} with B3LYP/6-31** and their electron density cubes mapped with ESP²⁹ (electrostatic potential charge values at chelating nitrogen atoms: for quinoline, −0.410; for quinoxaline, −0.197). The nitrogen atom in **1a** is a better donor and should form a more stable chelate as compared with **2a**. For more details, see the ESI part.

literature values of dissociation constants measured for protonated nitrogen bases: quinoline²⁷ and quinoxaline.²⁸ Surprisingly, quinoxaline is *more than 4 pK_a units less basic* than quinoline in H₂O. Since the Brønsted basicity should correlate with ligand donor properties, tremendous differences between the properties of these heterocycles may reveal differences between the activities of complexes **1a** and **2a**.

This result is in accord with the electronic effects of a chelate donor on catalytic activity described by us for Hoveyda second-generation catalyst analogues.^{5,6} Otherwise *for the first time* we describe the influence of electronic effect on unexplored trans to cis isomerization as being in the direction opposite to activity trends.^{30,31} This may be attributed to an impediment of the less nucleophilic nitrogen atom to coordinate to the ruthenium center

(27) (a) For quinoline, pK_a = 4.9 in H₂O at 25 °C: Boraei, A. A. *Monatsh. Chem.* **1994**, *125*, 869. (b) For quinoline, pK_a = 4.8 in H₂O at 25 °C: King, J. F.; Hillhouse, J. H.; Skonieczny, S. *Can. J. Chem.* **1984**, *62*, 1977.

(28) For quinoxaline, pK_a = 0.7 in H₂O at 25 °C: Goethals, M.; Czarnik-Matusiewicz, B.; Zeegers-Huyskens, T. *J. Heterocycl. Chem.* **1999**, *36*, 49.

(29) Electron density cubes from total SCF density (isoval = 0.0004; mapped with ESP) were generated with: *GaussView 3.0*; Gaussian, Inc., Wallingford, CT (www.gaussian.com).

(30) The magnitude of the observed effect of carbon-to-nitrogen substitution on isomerization and metathesis processes seems to be relatively small, as compared to, for example, differences of Brønsted basicities of chelating nitrogen atoms in ligands (the difference in ligand properties exhibits a bit more pronounced effect on the rate of isomerization in this case). However, the limited data impeded us from speculating on deeper mechanistic reasons for this observation (however, for some structural considerations, see ref 31). We wish to thank a reviewer for drawing our attention to this issue.

(31) Except for the electronic effect of chelating nitrogen atoms and insignificant differences in the geometries of ligands, two additional factors that differ in **1b** and **2b** have to be considered; namely, π -stacking of the chelating nitrogen heterocycle with a mesityl ring of the NHC ligand³² and the effect of the second nitrogen atom in **2b** on the dipole distribution as compared to the case for **1b**. The first effect cannot be substantial, since, on the basis of the X-ray structure of **1b**, the π -stacking interaction exists between one of the mesityls of the NHC ligand and the carbocyclic ring of quinoline. Thus, the presence of an additional nitrogen atom in the second heterocyclic ring (as in the quinoxaline fragment of **2b**) can probably be omitted. The latter effect, however, can more substantially stabilize the cis complex **2b**, as compared to **1b**, and thus can influence the equilibrium with the trans isomer. According to the quantum mechanics calculations²² in the gas phase the cis isomer of a similar complex is less stable than the trans isomer, due to the unfavorable dipole moment arising from polarized Ru–Cl bonds (in the trans complex the dipole moments of Ru–Cl bonds mutually cancel). However, this effect is diminished by solvents with high dielectric constant, e.g. dichloromethane, where the cis form predominates in an equilibrium. The presence of the second nitrogen atom in the quinoxaline ring in **2b** creates a dipole moment that is opposite to that of the equatorial chloride ion and, thus, partially reduces the total polarity of this complex. In fact, although **2b** should be slightly better stabilized as compared to **1b**, it is formed at a significantly lower rate.

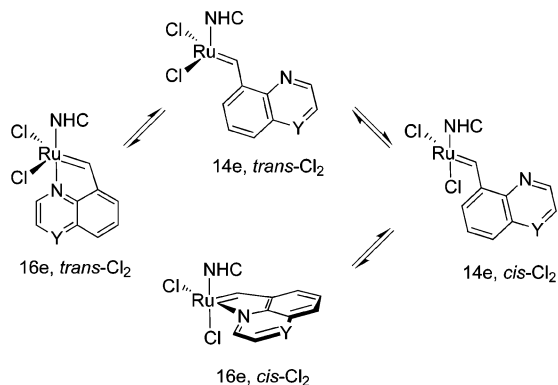


Figure 11. Postulated mechanism of the isomerization of **1a** and **2a** (based on ref 22).

at an equatorial position in place of the negatively charged chloride anion as present in the *trans* isomer.

According to quantum mechanics calculations²² of similar pyridine complexes, simplified mechanistic pattern of isomerization process is as shown in Figure 11: the *trans*-dichloro complex (**1a** or **2a**) dissociates to form an 14-electron intermediate, which isomerizes to another 14-electron intermediate with a *cis*-dichloro arrangement of chloride ligands, and finally recoordination of the chelating nitrogen atom gives the *cis*-dichloro complex (**1b** or **2b**, respectively).

On the basis of the observed activity trends one may assume that in the first step of this process (**16e trans-Cl₂** → **14e trans-Cl₂**) **2a** dissociates more quickly than **1a**.³³ However, the structure of the arylidene ligand should show little influence on the second process (**14e trans-Cl₂** → **14e cis-Cl₂**), if any. Thus, the much lower rate of isomerization of **2a** as compared to that of **1a** has to depend on the last, rate-determining step—the formation of the *cis* complex **1b** or **2b**.

Conclusions

We have presented a new family of second-generation Grubbs type catalysts which are perfectly stable. The rate of the *trans* to *cis* dichloro isomerization process was measured for the first time and can help to formulate the mechanistic concept of this process. Further explorations into the use of these complexes in ring-opening metathesis polymerizations (ROMP) are ongoing.

Experimental Section

8-Vinylquinoline. In a Schlenk tube was placed solid Pd(PPh₃)₂Cl₂ (0.015 g, 5 mol %), and a solution of 8-quinolyl trifluoromethanesulfonate (0.122 g, 0.44 mmol) in DMF (2 mL) was added under argon. Neat Bu₃SnCH=CH₂ (0.154 g, 0.484 mmol) was added via syringe, and the resulting solution was heated to 100 °C for 7 h. After the mixture was cooled to room temperature, the solvent was evaporated to dryness and solid KF (0.40 g) and ethyl acetate (2 mL) were added to the residue. The mixture was stirred at room temperature for 2 h and evaporated to dryness. To the residue were added AcOEt (15 mL) and water (10 mL). The organic phase was separated, and the aqueous phase was extracted with AcOEt (3 × 15 mL). The combined extracts were dried and

evaporated. The crude product was purified by column chromatography (10% ethyl acetate in cyclohexane) to give 0.0392 g (54%) of 8-vinylquinoline as a yellow oil. ¹H NMR (500 MHz, CDCl₃): δ 5.53 (dd, *J* = 11.07, 1.49 Hz, 1H), 5.94 (dd, *J* = 1.65, 17.65 Hz, 1H), 7.39–8.15 (m, 6H), 8.95 (s, 1H) ppm. MS (EI; *m/z* (relative intensity)): 40 (2), 63 (2), 77 (6), 101 (2), 126 (3), 127 (6), 128 (3), 153 (3), 154 (74, M⁺).

5-Vinylquinoxaline. In a Schlenk tube was placed a solution of 5-bromoquinoxaline (0.069 g, 0.33 mmol) in toluene (1.5 mL), and solid Pd(PPh₃)₄ (0.011 g, 3 mol %) was added under argon. Neat Bu₃SnCH=CH₂ (0.1151 g, 0.363 mmol) was added from a syringe, and the resulting solution was heated at 110 °C for 3 h. After the mixture was cooled to room temperature, the solvent was evaporated to dryness and solid KF (0.44 g) in ethyl acetate (1.5 mL) was added to the residue. The mixture was stirred at room temperature for 2 h, and the solvent was evaporated to dryness. To the residue were added AcOEt (15 mL) and water (10 mL). The organic phase was separated, and the aqueous phase was extracted with AcOEt (3 × 15 mL). The combined organic extracts were dried and evaporated. The crude product was purified by column chromatography (5% ethyl acetate in cyclohexane) to give 0.040 g (76%) of 5-vinylquinoxaline as a yellow oil. IR (film): ν 3435, 3085, 3025, 2924, 2851, 2668, 1924, 2851, 1679, 1621, 1599, 1574, 1488, 1470, 1448, 1353, 1216, 1200, 1145, 1043, 1009, 914, 865, 840, 765, 515, 449 cm⁻¹. ¹H NMR (200 MHz, CDCl₃): δ 5.50–5.60 (dd, *J* = 11.07, 1.26 Hz, 1H), 5.95–6.10 (dd, *J* = 1.43, 17.88 Hz, 1H), 7.65–8.08 (m, 5H), 8.85 (s, 1H) ppm. ¹³C NMR (50 MHz, CDCl₃): δ 116.9, 125.7, 128.9, 129.8, 131.7, 136.8, 140.6, 142.9, 143.9, 144.8. MS (EI; *m/z* (relative intensity)): 41 (8), 67 (22), 76 (21), 102 (4), 128 (3), 155 (25, M⁺). Anal. Calcd for C₁₀H₁₃O₂ (156.188): C, 76.90; H, 5.16; N, 17.94. Found: C, 76.66; H, 5.36; N, 18.07.

Preparation of Catalyst 1a. A Schlenk tube equipped with a stirring bar was charged with second generation Grubbs catalyst (102 mg; 0.12 mmol) and CuCl (13 mg, 0.12 mmol). The tube was flushed with argon and charged with anhydrous CH₂Cl₂ (3 mL). 8-Vinylquinoline (0.132 mmol; 20.5 mg) in anhydrous CH₂Cl₂ (3 mL) was then added, and the reaction mixture was heated to 40 °C for 20 min. The reaction mixture was concentrated to dryness, and the residue was dissolved in AcOEt. The precipitate was filtered off, and the solution was evaporated to dryness. The residue was redissolved in AcOEt and the solution was passed through a Pasteur pipet containing a small amount of silica gel and evaporated to dryness. The solid was collected and washed a few times with AcOEt and with cold *n*-pentane to give **1a** as a green solid (0.12 mmol; 62 mg, 89%). Crystals suitable for X-ray analysis were obtained by laying hexane over a solution of the catalyst in benzene and left for a few days at room temperature. IR (KBr): ν 3436, 2950, 2915, 2735, 1733, 1607, 1589, 1496, 1481, 1417, 1401, 1379, 1379, 1318, 1263, 1211, 1175, 1154, 1133, 1095, 1035, 992, 915, 850, 833, 792, 773, 748, 646, 618, 592, 578, 512, 426, 414 cm⁻¹. ¹H NMR (500 MHz, CD₂Cl₂): δ 2.46–2.51 (m, 18H), 4.14 (s, 4H), 7.11 (s, 1H), 7.26–8.25 (m, 4H), 8.36 (dd, *J* = 1.3, 3.6 Hz, 1H), 17.05 (s, 1H) ppm. ¹³C NMR (125 MHz, CD₂Cl₂): δ 19.4, 21.3, 52.1, 116.8, 123.5, 124.6, 129.3, 129.7, 131.7, 134.0, 137.1, 139.0, 142.7, 144.4, 146.3, 148.6, 151.7, 155.7, 212.9, 288.0 ppm. MS (ESI; *m/z*): 625 [M – Cl + CH₃CN]⁺. The molecular formula was confirmed by comparing the theoretical and experimental isotope patterns—found to be identical within the experimental error limits.

Preparation of Catalyst 1b. The *cis* isomer was prepared by dissolving **1a** (62 mg, 0.120 mmol) in CH₂Cl₂ (1 mL). The solution was left for 3 days at room temperature under argon. After this time the solution was evaporated to dryness. The residue was washed with AcOEt/*n*-pentane and then CH₂Cl₂/*n*-pentane to obtain a dark green powder (48%, 30 mg). Crystals suitable for X-ray analysis were obtained by laying *n*-hexane over a solution of the

(32) For the postulated π-face interactions in Ru carbene complexes containing NHC ligands, see: (a) Fürstner, A.; Ackermann, L.; Gabor, B.; Goddard, R.; Lehmann, C. W.; Mynott, R.; Stelzer, F.; Thiel, O. R. *Chem. Eur. J.* **2001**, *7*, 3236. (b) Süßner, M.; Plenio, H. *Chem. Commun.* **2005**, 5417.

(33) In this context it is necessary to presume that the tested substrates do not activate the catalysts or activate them to a similar extent.

catalyst in CH₂Cl₂ at room temperature. IR (KBr): ν 3447, 2922, 2854, 2735, 1819, 1731, 1628, 1607, 1588, 1570, 1496, 1481, 1437, 1400, 1380, 1316, 1291, 1263, 1209, 1176, 1131, 1036, 987, 914, 845, 817, 796, 781, 742, 696, 639, 624, 577, 477, 453, 427 cm⁻¹. ¹H NMR (500 MHz, CDCl₃): δ 2.90–1.40 (m, 18H), 4.30–3.60 (m, 4H), 6.15–8.05 (m, 4H), 8.14 (d, J = 8.1 Hz, 1H), 8.30 (d, J = 4.9 Hz, 1H), 17.44 (s, 1H) ppm. ¹³C NMR (125 MHz, CDCl₃): δ 19.1, 21.2, 51.2, 119.1, 123.5, 124.4, 127.7, 129.1, 129.5, 129.7, 130.0, 130.1, 133.2, 136.0, 140.3, 151.2, 152.8, 157.6, 217.7, 282.3 ppm.

Preparation of Catalyst 2a. The second-generation Grubbs catalyst (101.9 mg, 0.120 mmol), CuCl (13.1 mg, 0.132 mmol), and CH₂Cl₂ (3 mL) were placed in a Schlenk tube. Then a solution of 5-vinylquinoxaline (20.5 mg, 0.132 mmol) in CH₂Cl₂ (3 mL) was added, and the resulting solution was stirred under argon at 40 °C for 20 min. From this point forth, all manipulations were carried out in air with reagent-grade solvents. The reaction mixture was concentrated under vacuum, and the resulting material was dissolved in AcOEt (ca. 10 mL). A small amount of white solid was filtered off, and the filtrate was concentrated under vacuum. The product was purified by column chromatography on silica gel using AcOEt as eluent. Evaporation of the solvent and crystallization from CH₂Cl₂ and *n*-pentane afforded **2a** as a deep green powder (52 mg, 72%). IR (KBr): ν 3439, 2953, 2920, 2855, 2735, 1943, 1730, 1630, 1607, 1574, 1484, 1420, 1379, 1264, 1202, 1149, 1080, 1035, 927, 910, 853, 834, 774, 716, 646, 578, 514, 473, 419 cm⁻¹. ¹H NMR (500 MHz, CDCl₃): δ 2.38–2.50 (m, 18H), 4.16 (s, 4H), 7.08 (s, 1H), 7.35–7.62 (s, 1H), 8.38 (m, 1H), 8.45 (d, J = 2.3 Hz, 1H), 8.57 (d, J = 2.2 Hz, 1H), 17.00 (s, 1H) ppm. ¹³C NMR (125 MHz, CDCl₃): δ 19.2, 21.2, 51.7, 116.6, 124.0, 126.5, 128.7, 129.5, 134.9, 136.2, 138.5, 138.8, 141.6, 144.2, 145.6, 147.9, 156.2, 210.5, 288.2 ppm. MS (ESI; m/z): 626 [M – Cl + CH₃CN]⁺. The molecular formula was confirmed by comparing the theoretical and experimental isotope patterns—found to be identical within the experimental error limits.

General Procedure for the Preparation of Catalyst 2b. Catalyst **2b** (55 mg, 0.115 mmol) was prepared by dissolving **2a** in CH₂Cl₂ (2 mL). The solution was left for 16 days at room

temperature under argon, and the solvent was evaporated to dryness. The residue was washed with a mixture of solvents, CH₂Cl₂ and *n*-pentane, to obtain **2b** as a dark brown powder (62%, 34 mg). IR (KBr): ν 3436, 2921, 2855, 1942, 1725, 1630, 1593, 1483, 1442, 1404, 1379, 1314, 1266, 1219, 1195, 1154, 1079, 1034, 929, 907, 853, 823, 805, 768, 717, 667, 645, 630, 577, 474, 443, 420 cm⁻¹. ¹H NMR (200 MHz, CDCl₃): δ 1.84–2.51 (m, 18H), 4.0–4.15 (s, 4H), 7.08 (s, 4H), 7.50–7.54 (m, 2H), 7.60–7.58 (m, 1H), 8.38 (m, 1H), 8.48 (d, J = 4.2 Hz, 1H), 17.30 (s, 1H) ppm.

RCM and Enyne Reactions. The catalyst (5 mol %, 0.018 mmol) was added to a solution of a substrate (0.350 mmol) and an internal standard (*n*-dodecane) in CH₂Cl₂ (17.5 mL). The reaction was run at room temperature under Ar, and aliquots were taken after 15 min, 30 min, 45 min, 60 min, 1.5 h, 2 h, 4 h, 6 h, and 24 h and analyzed by GC.

Acknowledgment. We wish to thank Prof. Dr. Siegfried Blechert (Technical University of Berlin) for information on his related work and Dr. Gerald Dräger (Institut für Organische Chemie, Universität Hannover) for excellent ESI measurements of complexes **1** and **2**. A.S. acknowledges the Institute of Organic Chemistry, Polish Academy of Sciences, for a conference allowance.³⁴ Authors thank Dr. Iwona Justyniak (Institute of Physical Chemistry PAS, Warsaw) and the Crystallographic Unit of the Physical Chemistry Laboratory at the Chemistry Department of the University of Warsaw for solving of X-ray structures.

Supporting Information Available: Text, tables, figures, and CIF files giving key details of the X-ray structures and NMR and ESI spectra. This material is available free of charge via the Internet at <http://pubs.acs.org>.

OM060091U

(34) Part of this work has been presented as a poster: Szadkowska, A.; Barbasiewicz, M.; Grela, K. Synthesis and application of new latent ruthenium carbene catalysts. European Congress of Young Chemists "YoungChem 2005", Rydzyna, Poland, October 12–16, 2005.